Vortex Ring Dynamics in the Unitary Fermi Gas

Michelle Kelley
University of Washington, Seattle
Physics REU Program
Mentors: Michael Forbes and Aurel Bulgac

September 4, 2013

Abstract

A recent article, Yefsah *et al.*, **Nature** 499, 426 (2013) [1], reported an unusual excitation in a harmonically trapped unitary Fermi gas. The experiment imprints a domain wall in the trap resulting in oscillations that have periods an order of magnitude longer than the trapping period. The authors interpretted the results as 'heavy solitons,' but vortex rings provide a more natural explanation of the observed periods. This paper reports the results of simulations of a vortex ring in a harmonic trap to mimic the experiment, using the density functional theory, specifically the extended Thomas-Fermi Gross-Pitaevskii model. Vortex rings in harmonic traps experience long oscillatory periods, comparable to the oscillations found in the experiment. It was found that the oscillatory period of the vortex ring increases with the aspect ratio of the trap, and decreases for oscillations with smaller amplitudes of oscillation. Additionally, oscillations experienced anti-damping when the system was not allowed to cool completely, matching well with the experiment's observed anti-damped oscillations.

1 Introduction

The Bardeen-Cooper-Schriefer (BCS) to Bose Einstein Condensation (BEC) crossover in ultracold Fermi gases provides a model system where theoretical techniques can be tested against experiments. In dilute Fermi gases, the range of the potential is much less than the interparticle spacing, k_F^{-1}. The interaction of the system can be characterized by the dimensionless parameter $(k_F\, a)^{-1}$, where a is the scattering length. In the BCS limit, the scattering length is negative and $(k_F\, a)^{-1} \to -\infty$. The system is weakly interacting and the atoms form long-range Cooper pairs. In the BEC limit, the scattering length is positive and $(k_F\, a)^{-1} \to +\infty$. The atoms pair up to form tightly bound dimers, which behave like bosons. For the ground state of the ultracold Fermi gas, there is a smooth crossover from the BCS limit to the BEC limit [2].

The BCS-BEC crossover can be realized experimentally by adjusting the scattering length through an external magnetic field

$$a(B) \sim \frac{C}{B - B_{\text{res}}} \tag{1}$$

where B is the externally applied magnetic field and $B_{\rm res}$ is the resonant magnetic field of the system. The Unitary limit occurs at the Feshbach resonance and $a \to \infty$. The parameter $(k_F\, a)^{-1} \to 0$ and all length scales drop out of the problem and a theory is obtained that is set only by the particle density. The unitary Fermi gas (UFG) exhibits remarkable properties, emerging from scale invariance, and creates an excellent opportunity to make quantitative comparisons between theory and experiment. Furthermore, many-body methods can be tested so they can be applied to similar systems such as dilute neutron matter in neutron stars [2].

2 Experimental Puzzle

A recent experiment conducted at the MIT-Harvard Center for Ultracold Atoms reported the observation of an unexpected excitation in a harmonically trapped UFG [1]. The experiment took $\sim 10^5$ ^{6}Li atoms in an elongated harmonic trap and imprinted a laser beam on half of the trap, twisting the phase of half of the wave function. The experiment reported long oscillations of slowly moving 'solitons,' having periods an order of magnitude longer than what was expected from previous theories.

The observed oscillations cannot be resolved *in situ*, and instead a procedure was used to image the oscillations. The procedure included eliminating the harmonic trap, allowing the gas cloud to expand, and taking an image of the expanded gas cloud. The images show planar depletions which the authors interpreted as solitons.

However, vortex rings provide a more natural explantation for the long observed oscillations. This paper reports the results of simulations involving vortex rings in harmonic traps that mimic the experimental conditions [1].

3 Methods

3.1 The Gross-Pitaevskii Model

Dynamics simulations of the vortex rings are performed using Density Functional Theory (DFT). The Thomas-Fermi extension of the Gross-Pitaevskii equation well describes the unitary Fermi gas in the superfluid regime

$$i\hbar\partial_t\Psi = \left(\frac{-\hbar^2\nabla^2}{4m_F} + 2V_{\rm ext} + 2\partial_n\mathcal{E}(n,a)\right)\Psi \tag{2}$$

where $n = 2|\Psi|^2$ is the fermion number density and $\mathcal{E}(n,a)$ is the energy-density as a function of scattering length a, which can be manipulated with time and must be fit to the equation of state. The QMC equation of state of a dilute Fermi gas has been parametrized for positive scattering lengths [3].

$$\mathcal{E}(n,a) = \frac{3}{5}\varepsilon n\xi\frac{\xi + x}{\xi + x(1+\zeta) + 3\pi\xi x^2} - \frac{\hbar^2}{2ma^2}n \tag{3}$$

The somewhat odd factors of two arise because there are two fermions per dimer. This is a bosonic model, thus only one wave function is needed as opposed to other density functional theories such as the Time Dependent Superfluid Local Density Approximation (TDSLDA) which is much more computationally expensive [3].

3.2 Time Evolution

The system is evolved using the split operator method.

$$\Psi(t+\delta_t) = (e^{-iK\delta_t/2} e^{-iV\delta_t} e^{-iK\delta_t/2})\,\Psi(t) + \mathcal{O}(\delta_t^3) \tag{4}$$

The error scales with $\mathcal{O}(\delta_t^3)$ resulting from splitting the kinetic term. The exponentials must be computed to sufficiently high order to have this error scaling. Since a bosonic model is being used, the kinetic term is constant and diagonal in momentum space while the potential is diagonal in position space and the exponents can be evaluated exactly. More careful evaluation is required if the potential depends on ψ, if the potential is not constant through δ_t, and for Fermionic DFTs.

Applying the potential only affects the phase of the wave function, leaving the density constant. Since the vortex is a spinning object, the phase of the wave function twists around it. The whirling of the phase through time does not contain physical significance, and it can be advantageous to subtract the chemical potential, $\langle\psi|H|\psi\rangle/\langle\psi|\psi\rangle$, from the effective potential.

To cool the system, the wave function is evolved with complex time. After cooling, the system is evolved with real-valued time steps.

3.3 Imprinting and Tracking a Vortex

To imprint a vortex, a pinning potential is introduced to the wavefunction

$$V_{\text{ring}} = V_{\text{pin}} \exp\left(-\frac{(r-R)^2 + (z-z_0)^2}{2\,(r_{\text{pin}})^2}\right) \tag{5}$$

where V_{pin} determines the strength of the pinning potential and r_{pin} determines the thickness of the pinning potential. The pinning strength, V_{pin}, is a step function and goes to zero by the time the system is done cooling.

To extract the period of the vortex as it oscillates about the trap, the trajectory of the vortex is tracked. This is done through a least squares fit, fitting the wave function to

$$\psi = \frac{(z+ir) - (z_0+iR)}{2\xi^2 + |(z+ir) - (z_0+iR)|^2}|\psi_0| \tag{6}$$

where ψ_0 is the wave function of the gas cloud in the trap without a vortex and ξ is the healing length of the vortex. The axial and radial position of the vortex are given by z_0 and R respectively. The fitting function is sensitive and requires an accurate guess to return the location of the vortex. Initially, the guess is given by the position of the pinned vortex and as the wavefunction is evolved, the guess is provided from a third-order polynomial fit of the previous five vortex locations.

4 Results

The period of oscillation was found to depend on the aspect ratio of the trap as well as the imprint location of the vortex. The simulations exploited the axial symmetry

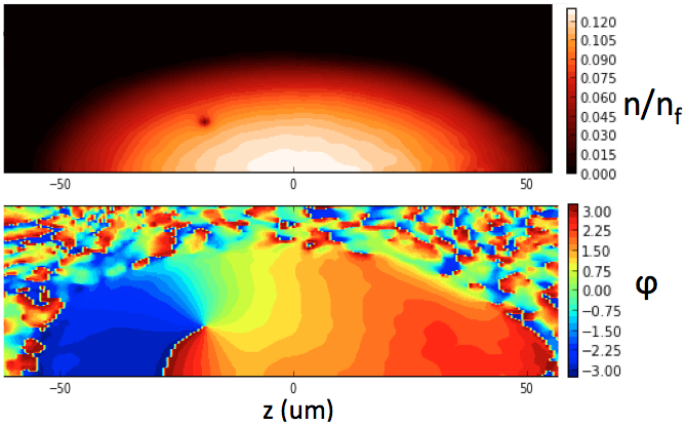

Figure 1: Image in the R-z-plane of a preliminary simulation of the harmonically trapped superfluid provided as a reference for the reader. The top plot shows the density profile of the system, and the bottom plot shows the corresponding phase. The vortex can be seen as a density depletion, and the phase around the vortex twists from 0 to 2π.

Table 1: Imprinting the vortex at different radial positons

Imprint Location	Period	Amplitude
$R_0 = 0.20\ R_\perp$	$T = 8.6\ T_z$	$\sim 0.45\ R_z$
$R_0 = 0.30\ R_\perp$	$T = 9.9\ T_z$	$\sim 0.35\ R_z$
$R_0 = 0.40\ R_\perp$	$T = 10.7\ T_z$	$\sim 0.15\ R_z$
$R_0 = 0.50\ R_\perp$	$T = \ 11\ T_z$	$\sim 0.05\ R_z$

of the system, thus 2-dimensional simulations were ran and could be extended for 3-dimensional results. The simulations were performed for a slice down the middle of the harmonic trap, using the 2-dimensions for the axial and radial direction. A slice of a vortex ring is a vortex-antivortex pair, and only one vortex is shown in the simulations due to the radial coordinates used. Figure 1 illustrates how the simulations appeared.

The oscillation period depended on the amplitude of the oscillations. This dependence was found by imprinting the vortex at different radial positions of the trap, and the results can be seen in Table 1 and Figure 2. The oscillations with larger amplitudes corresponded to longer periods of oscillation. At the critical radius, the vortex is stationery which was found to happen for $\sim R_0 = 0.49 R_\perp$. The parameter $R_\perp$ is the TF radius of the gas cloud, and R_z is its axial length. Vortices imprinted at radii greater than the critical radius experienced the same trajectory as imprinted the same distance below the critical radius.

The period of the oscillation also depends on the aspect ratio, λ, of the trap. The aspect ratio is the ratio of the axial trapping period to the radial trapping period, $\lambda = T_z/T_\perp$. Simulations were ran at the same three aspect ratios as reported in the experiment, $\lambda = 3.3,\ 6.2,\ 15.0$. Table 2 shows the oscillations of a vortex imprinted at

Table 2: Observed oscillations and particle numbers for the three aspect ratios

Aspect Ratio	Period	Particle number
$\lambda = 3.3$ ($T_z = 47.6$ms)	$T = 9.9\ T_z$	$N = 461\,512$
$\lambda = 6.2$ ($T_z = 89.4$ms)	$T = 8.4\ T_z$	$N = 460\,796$
$\lambda = 15.0$ ($T_z = 216.4$ms)	$T = 6.7\ T_z$	$N = 461\,530$

$R_0 = 0.30 R_\perp$ for the three aspect ratios. The period of oscillation are shown in units of the trapping period, and the periods increased as the aspect ratio decreased.

Simulations were also ran where the system was insufficiently cooled, causing the oscillation to become anti-damped. Anti-damped oscillations were seen in the experiment when conducted at higher temperatures. In the experiment, the period was found to remain roughly constant within the experimental uncertainty. Here, it is found that anti-damped systems have periods that decrease as the amplitude of oscillation increases. Figure 3 shows oscillations for a trap of $\lambda = 6.2$ for a completely cooled system and an insufficiently cooled system.

5 Conclusion

The period of oscillation of a vortex ring in a harmonic trap was found to depend on the initial imprint location of the vortex as well as the aspect ratio of the trap. Shorter aspect ratios corresponded to longer periods of oscillation with respect to the trapping period. The oscillatory period was also found to depend on the amplitude of oscillation, which was shown by imprinting the vortex at different locations. Larger amplitudes of oscillation corresponded to shorter periods. Finally, when the system was insufficiently cooled the amplitude of oscillation increased and the period decreased. This final result matched well with the anti-damping observed in [1].

This material is based on work supported in part by NSF Physics REU. Any opinions, findings, conclusions, or recommendations expressed in this material are those of the author and do not necessarily reflect those of NSF.

References

[1] Zwerger, W. (2012). *The BCS-BEC crossover and the unitary Fermi gas.* Heidelberg: Springer.

[2] T. Yefsah, A. T. Sommer, M. J. H. Ku, L. W. Cheuk, W. Ji, W. S. Bakr, and M. W. Zwierlein, Nature 499, 426 (2013), arXiv:1302.4736 [cond-mat].

[3] A. Bulgac, M. M. Forbes, M. M. Kelley, K. J. Roche, and G. Wlazlowski, arXiv:1306.4266v2 [cond-mat.quant-gas]

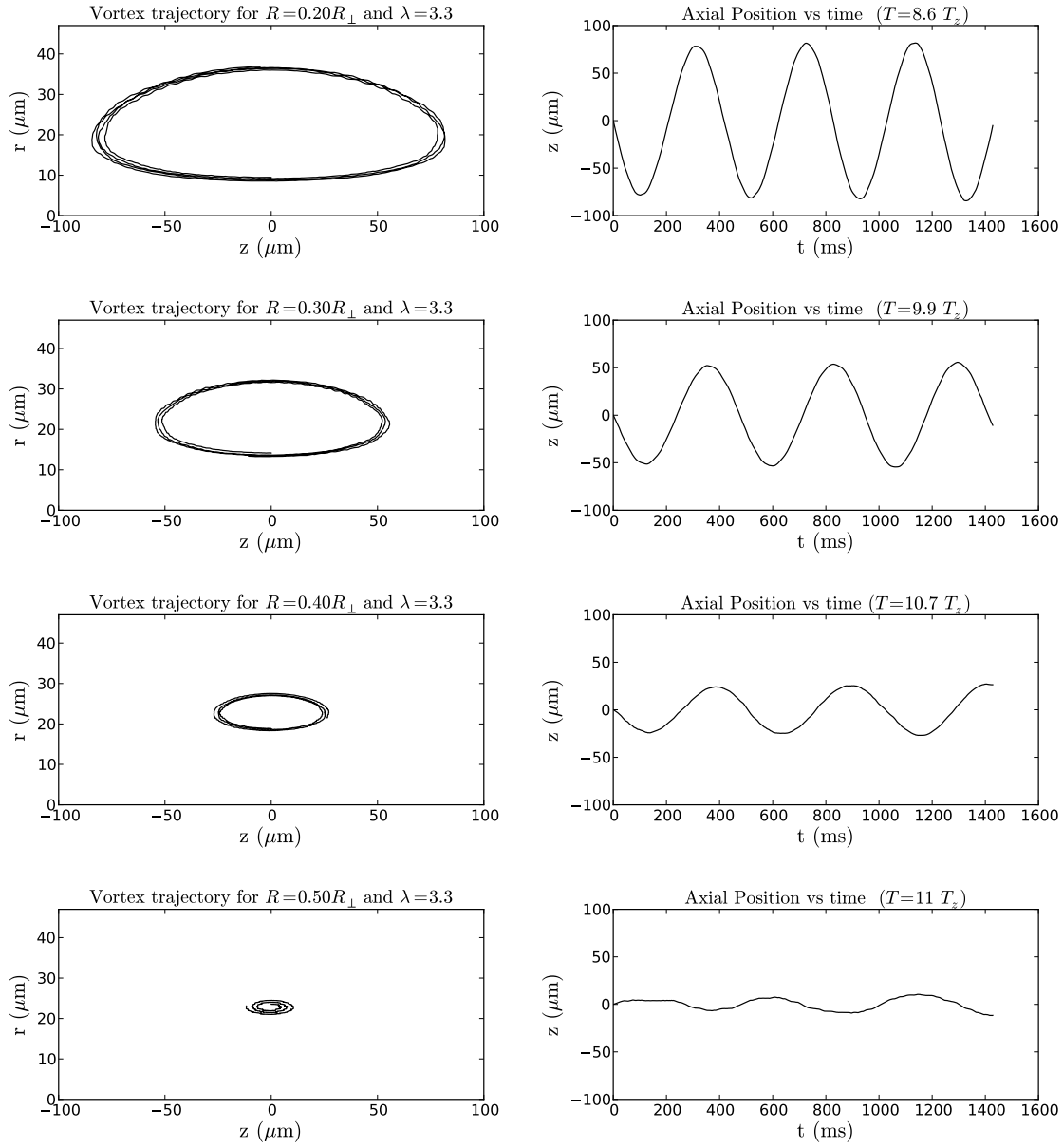

Figure 2: The left column displays the different trajectories of a vortex ring in the R-z plane, while the right column shows the time dependence of the axial position of the vortex ring. The fourth row show an example of an almost stationary vortex ring. The radius of a stationary vortex ring is $\approx 0.49R_\perp$, where $R_\perp$ is the TF radius of the cloud

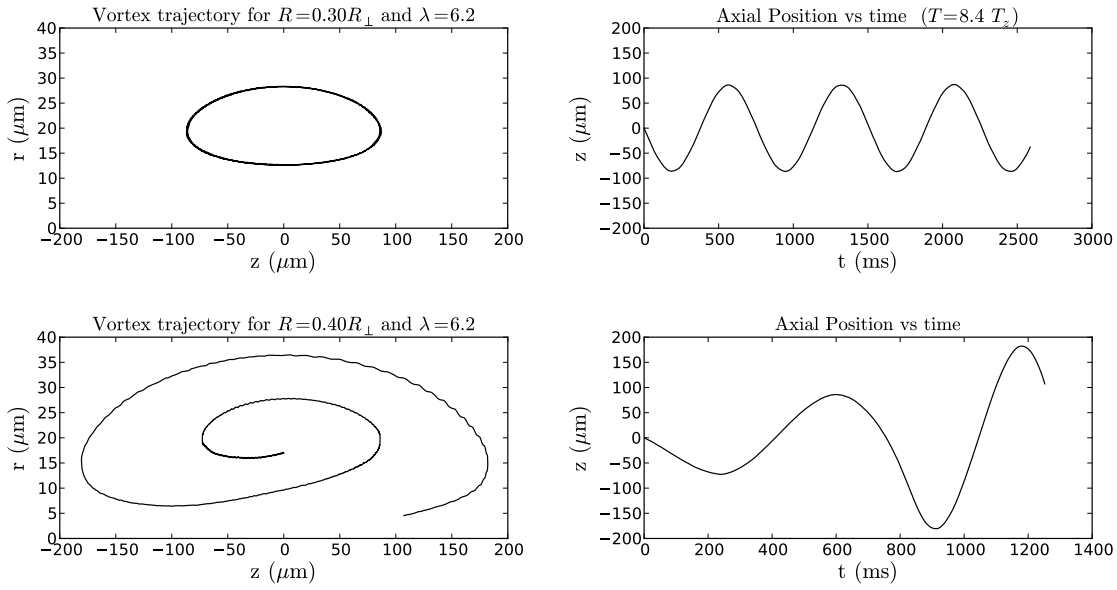

Figure 3: The left column displays the different trajectories of a vortex ring in the R-z plane, while the right column shows the time dependence of the axial position of the vortex ring. Both simulations were ran with an aspect ratio $\lambda = 6.2$. The vortex in the top plot was allowed to cool completely, and the vortex in the bottom plot was not. It can be seen that the system will experience anti-damped oscillations when the system is insufficiently cooled.